

JUN 19 2007

REPORT DOCUMENTATION PAGE			Form Approved OMB No. 0704-0188		
<p>The public reporting burden for this collection of information is estimated to average 1 hour per response, including the time for reviewing instructions, searching existing data sources, gathering and maintaining the data needed, and completing and reviewing the collection of information. Send comments regarding this burden estimate or any other aspect of this collection of information, including suggestions for reducing the burden, to Department of Defense, Washington Headquarters Services, Directorate for Information Operations and Reports (0704-0188), 1215 Jefferson Davis Highway, Suite 1204, Arlington, VA 22202-4302. Respondents should be aware that notwithstanding any other provision of law, no person shall be subject to any penalty for failing to comply with a collection of information if it does not display a currently valid OMB control number.</p> <p><b>PLEASE DO NOT RETURN YOUR FORM TO THE ABOVE ADDRESS.</b></p>					
1. REPORT DATE (DD-MM-YYYY) 12-06-2007	2. REPORT TYPE Final Report		3. DATES COVERED (From - To) Dec 2003- Nov 2006		
4. TITLE AND SUBTITLE Atomistic Modeling of Advanced Intermetallic Alloys			5a. CONTRACT NUMBER FA9550-04-1-0017		
			5b. GRANT NUMBER		
			5c. PROGRAM ELEMENT NUMBER		
			5d. PROJECT NUMBER		
6. AUTHOR(S) Dr. Yuri Mishin			5e. TASK NUMBER		
			5f. WORK UNIT NUMBER		
			8. PERFORMING ORGANIZATION REPORT NUMBER 200661		
7. PERFORMING ORGANIZATION NAME(S) AND ADDRESS(ES) George Mason University 4400 University Drive Fairfax, VA 22030			10. SPONSOR/MONITOR'S ACRONYM(S) AFOSR		
9. SPONSORING/MONITORING AGENCY NAME(S) AND ADDRESS(ES) AF Office of Scientific Research 875 North Randolph Street, RM 3112 Arlington, VA 22203 <i>Brett Conner/NSA</i>			11. SPONSOR/MONITOR'S REPORT NUMBER(S)		
			12. DISTRIBUTION/AVAILABILITY STATEMENT Approved for public release; distribution unlimited.		
13. SUPPLEMENTARY NOTES					
14. ABSTRACT A fundamental study of structure, thermodynamic and kinetic properties of structural intermetallic alloys was performed by means of atomistic computer simulations. Gamma-gamma prime alloys of the Ni-Al system were chosen as model materials due to their high promise as structural alloys for high-temperature aerospace applications, such as superalloys for gas-turbine engines. The methodology included the construction of new interatomic potentials for multi-component systems, large-scale molecular dynamics and Monte Carlo simulations and other advanced methods. A new Nye-tensor method for the analysis of dislocation core structure in materials has been developed. The properties studied include atomic diffusion, dislocation behavior, structure and energy of generalized stacking faults in the gamma-prime phase, and energetics of inter-phase boundaries. The project provides new fundamental understanding of diffusion mechanisms in ordered intermetallic phases, understanding of dynamics of the locking-unlocking processes in moving dislocations during plastic deformation, and reliable data on interface energies in alloys. The results					
15. SUBJECT TERMS Computer modeling of metallic materials; high-temperature alloys; atomic diffusion; dislocations and plasticity.					
16. SECURITY CLASSIFICATION OF:			17. LIMITATION OF ABSTRACT UU	18. NUMBER OF PAGES 10	19a. NAME OF RESPONSIBLE PERSON Dr. Yuri Mishin
a. REPORT U	b. ABSTRACT U	c. THIS PAGE U			19b. TELEPHONE NUMBER (Include area code) 703-993-3984

# Final Report on the AFOSR grant No. FA9550-04-1-0017

This Report presents a summary of research conducted under the AFOSR grant No. FA9550-04-1-0017 “*Atomistic Modeling of Advanced Intermetallic Alloys*” (activity period 12/2003-11/2006) The goal of the project was to perform a fundamental study of structure, thermodynamic and kinetic properties of structural intermetallic alloys by means of atomistic computer simulations.  $\gamma/\gamma'$  alloys of the Ni-Al system were chosen as model materials. The Ni<sub>3</sub>Al-based  $\gamma'$  phase is a promising structural material for high-temperature applications. Two-phase  $\gamma$ - $\gamma'$  alloys serve as prototypes of Ni-base superalloys. The methodology used in this project includes the construction of new interatomic potentials, large-scale molecular dynamics (MD) and Monte Carlo simulations and other methods. The properties studied here include diffusion, structure and energy of generalized stacking faults (GSFs) in the  $\gamma'$  phase,  $\gamma/\gamma'$  inter-phase boundaries, and dislocation behavior in the  $\gamma'$  phase.

## 1 Interatomic potentials for the Ni-Al system

A new interatomic potential has been constructed within the embedded-atom method (EAM) formalism by fitting to both experimental and first-principles data [1]. The potential set includes accurate EAM potentials for Ni and Al and a cross-potential fit to first-principles energies of various Ni-Al compounds, including L1<sub>2</sub>-Ni<sub>3</sub>Al. The potentials have been tested by calculating a large variety of thermodynamic and physical properties of Ni, Al and Ni<sub>3</sub>Al, including phonon frequencies, thermal expansion, melting temperatures and heats, planar fault energies, point defect formation and migration energies, as well as experimental and first-principles formation energies of a series of Ni-Al compounds. The potentials has shown excellent performance for most properties tested. The Ni-rich part of the Ni-Al phase diagram has been calculated by the thermodynamic integration method in conjunction with grand-canonical Monte Carlo simulations. The reasonable agreement with experiment (Fig. 1) makes this potential applicable to atomistic simulations of  $\gamma$ - $\gamma'$  alloys.

## 2 Diffusion in NiAl and Ni<sub>3</sub>Al

Diffusion mechanisms operating in Ni<sub>3</sub>Al and NiAl have been established by large-scale MD simulations [1, 2]. Ni atoms diffuse in Ni<sub>3</sub>Al by exchanges with vacancies on the Ni-sublattice, whereas Al goes to the Ni sublattice, forms Al<sub>Ni</sub> antisites, and diffuses by exchanges with Ni vacancies. The diffusion mechanisms in NiAl are more complex. In this compound, deviations from stoichiometry on the Al-rich side are accommodated by structural vacancies on the Ni sublattice, whereas the Ni-rich side is dominated by Ni<sub>Al</sub> antisites [3]. It was found that the atomic configuration arising after a nearest-neighbor jump of a Ni vacancy is mechanically unstable. Because of this instability, the vacancy implements two sequential nearest-neighbor jumps as one collective transition involving two atoms. Such collective jumps initiate and complete six-jump vacancy cycles of a Ni vacancy. Thus, such cycles occur by either four or three

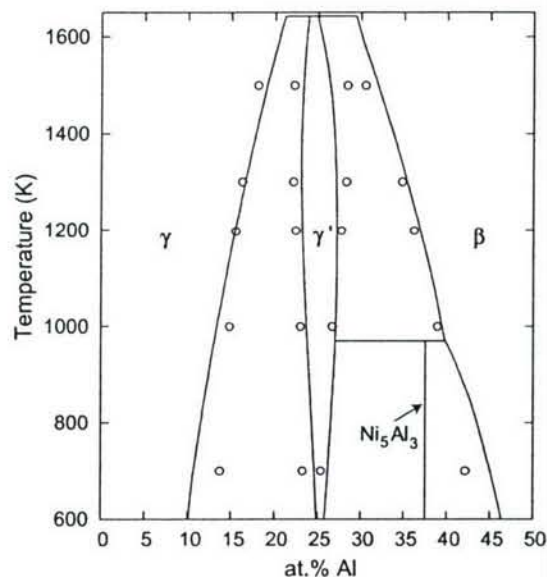


Figure 1: Ni-Al phase diagram calculated with the EAM potential developed in this project (points) in comparison with experiment (lines).

collective vacancy jumps, depending on whether the central configuration of the cycle is mechanically stable (as for [100] cycles) or unstable (as for [110] cycles). Calculations show that [110] cycles are energetically more favorable and should happen more frequently than [100] cycles. Next-nearest-neighbor vacancy jumps have diffusion rates comparable to experiment, suggesting that Ni diffusion on its own sublattice is an important diffusion mechanism in NiAl.

These findings have been verified by both static calculations and MD simulations [2]. Diffusion coefficients of Ni and Al in Ni<sub>3</sub>Al and NiAl by different mechanisms have been calculated by the kinetic Monte Carlo method as well as by direct MD simulations. The calculated diffusion coefficients compare well with experimental data. Together with our previous AFOSR work of diffusion in Ti-Al compounds, we now have a well established methodology for predictive diffusion calculations in transition-metal aluminides.

### 3 Interfaces in $\gamma$ - $\gamma'$ alloys

Interfaces play an important role in mechanical behavior of the  $\gamma'$  phase and  $\gamma$ - $\gamma'$  alloys of the Ni-Al system. The GSF energies dictate the dissociated structure of superdislocations in Ni<sub>3</sub>Al and thus determine their mobility. The energy of  $\gamma/\gamma'$  interfaces affects the coarsening kinetics of  $\gamma'$  particles in the  $\gamma$  matrix and creep resistance. Table 1 summarizes the interface energies at  $T = 0$  K computed with our EAM potential. They show very reasonable agreement with both experimental data and first-principles calculations [1].

It was established by grand-canonical Monte Carlo simulations that the (111) APB in stoichiometric Ni<sub>3</sub>Al shows a noticeable antisite disorder at high temperatures, whereas other GSFs

remain atomically sharp. At high temperatures,  $\gamma/\gamma'$  interfaces are diffuse, with the long-range order parameter changing gradually from almost 1 to zero over a 10-15 Å distance (Fig. 2). We are currently in the process of thermodynamic calculations of interface free energies as functions of temperature and chemical composition using thermodynamic integration methods in conjunction with Monte Carlo simulations.

Table 1: Energies (in  $\text{mJ}/\text{m}^2$ ) of generalized stacking faults and  $\gamma/\gamma'$  interfaces with different orientations in  $\text{Ni}_3\text{Al}$  calculated with the EAM potential [1]. APB: anti-phase boundary; CSF: complex stacking fault; SISF: superlattice intrinsic stacking fault.

(111) APB	(111) CSF	(111) SISF	(100) APB	(100) $\gamma/\gamma'$	(110) $\gamma/\gamma'$	(111) $\gamma/\gamma'$
252	202	51	80	46	28	12

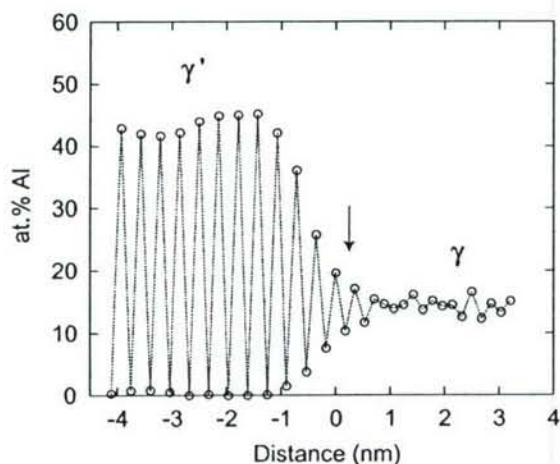


Figure 2: Concentration profile across a (100)  $\gamma/\gamma'$  interface in the binary Ni-Al system obtained by Monte Carlo simulations at 700 K. Individual points represent the Al concentration averaged over individual (200) layers. The arrow marks the initial ( $T = 0$ ) position of the interface.

## 4 The “prewetting” transition in $\gamma$ - $\gamma'$ alloys

Grand-canonical Monte Carlo simulations of APBs in Ni-rich  $\gamma'$  reveal 5-10 Å wide regions around the APB with greatly reduced long-range order and chemical composition approaching the composition of the  $\gamma$ -phase. As the bulk composition approaches the two-phase equilibrium line, the thickness of the  $\gamma$ -layer at the APB rapidly increases and eventually diverges. This local disordering of the APB must occur as a first-order interface phase transformation which can be classified among so-called “wetting” transitions, meaning that the APB becomes “wet” with the  $\gamma$  phase. A fact which is important for applications is that this transition can happen within the  $\gamma'$ -domain on the phase diagram, i.e. before the two-phase equilibrium is reached (“prewetting” transition).

We have studied the (111) APB prewetting transformation as a function of temperature and bulk composition. Only Ni-rich off-stoichiometries have been examined due to their relevance to  $\gamma$ - $\gamma'$  alloys. Ni is found to always segregate to this APB. Figure 3 displays the excess amount of Ni (relative to its bulk concentration, measured in the effective number of monolayers) as a function of the bulk composition at selected temperatures. Observe that the amount of Ni segregation increases with the degree of off-stoichiometry but decreases with temperature. At a constant temperature, the segregation curve has two stages. At small deviations from the stoichiometry, the segregation rapidly increases in a linear manner and reaches a saturation. At this stage the Ni concentration within the APB rapidly grows whereas the APB width remains almost constant and equal to approximately  $2d_{(111)}$ . By the end of this stage, the chemical composition within the APB comes very close to the equilibrium bulk composition of the  $\gamma$ -phase. At the second stage, the width of the APB region increases whereas its chemical composition remains nearly constant and close to the  $\gamma$ -phase composition. As the  $\gamma'$  bulk composition approaches the miscibility gap, the APB width rapidly grows and diverges. We are in the process of collecting enough data for constructing the entire prewetting line on the Ni-Al phase diagram.

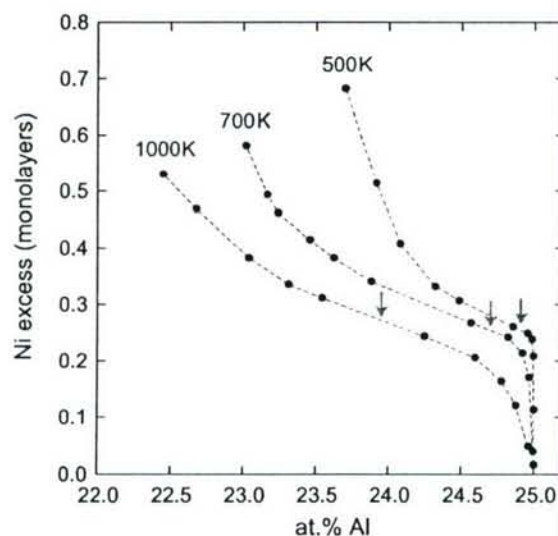


Figure 3: Ni segregation at the (111) APB in  $\text{Ni}_3\text{Al}$  alloys as a function of the bulk composition at selected temperatures. The left end of each curve is close to the bulk solubility limit. The arrows indicate the points of the “prewetting” transformation which turns the APB into a  $\gamma$  layer.

The APB prewetting transition can have significant consequences for the precipitation and coarsening of  $\gamma'$  particles in  $\gamma$ - $\gamma'$  alloys. If two growing particles can merge without forming an APB, they will readily do so. However, if an APB should result from the merger, such particles will not merge and will stay clear of each other. This effect imposes an additional resistance to the coarsening and is considered to be responsible for the discontinuous coarsening/rafting effect and other structural features of  $\gamma$ - $\gamma'$  alloys that affect mechanical properties. Dislocations

in the  $\gamma'$  phase can also be influenced by the APB prewetting effect. Screw superdislocations in  $\gamma'$  typically dissociate on a  $\{111\}$  plane with the formation of an APB bounded by two superpartials. The APB replacement by a  $\gamma$  layer must have a strongly impact on the dislocation mobility at high temperatures. This must affect the creep resistance of the  $\gamma'$  phase as well as superalloys.

## 5 Dislocations in the $\gamma'$ phase

$\text{Ni}_3\text{Al}$  is one of several  $\text{L1}_2$  intermetallic compounds which exhibit the yield-stress anomaly (YSA, the yield stress increases with temperature and shows a peak at a few hundred K). The YSA in  $\text{Ni}_3\text{Al}$  is accompanied by other unusual features of plastic deformation, such as (i) strong orientation dependence of the CRSS, (ii) tension-compression asymmetry, and (iii) small strain-rate sensitivity. The mechanism responsible for this behavior is believed to be thermally activated formation of dislocation locks arising by cross-slip of screw dislocations, or their segments, from the primary  $\{111\}$  plane to a cube  $\{001\}$  plane. After 30 years of studies of the YSA in  $\text{Ni}_3\text{Al}$ , there is still a number of unresolved problems. For example, there is no consensus about the exact structure of the dislocation locks. The mechanism of the small strain-rate sensitivity is not clear either. While dislocations in  $\text{Ni}_3\text{Al}$  have been studied by atomistic simulations in the past [4], all previous work was performed by static relaxation at 0 K. It thus dealt mostly with postulated dislocation structures and did not directly address the temperature effects, which are at the heart of the YSA.

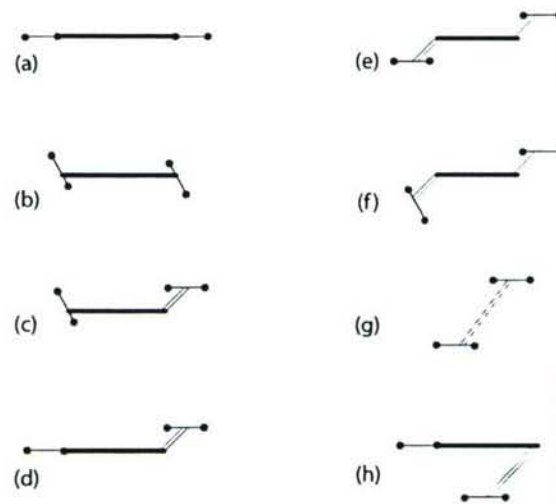


Figure 4: Superdislocation configurations observed by MD simulations. Thick lines –  $\{111\}$  APB, double thin lines –  $\{001\}$  APB, single thin lines – CSF, dots – Shockley partials. (a) Planar core; (b) Nonplanar core on octahedral planes. (c), (d) PPV lock of one partial; (e), (f) PPV locks of both partials; (g) Complete KW lock; (h) Incomplete KW lock found in this work.

We have started an extensive study of dislocation behavior in  $\text{Ni}_3\text{Al}$  by means of MD simu-

lations using the EAM potential developed in this project [1]. The advantage of MD is that the dislocation of interest evolves naturally under an applied shear stress and a chosen temperature. No a priori assumptions are made about its behavior; instead, the mechanisms of its motion are *deduced* from the simulations. Our simulations use a block containing up to half a million atoms. Taking advantage of massive parallel computing, MD simulation times up to several tens of nanoseconds have been achieved. Several temperatures (700-1300 K), stress levels (500-800 MPa) and strain rates have been tested. The initial configuration is always a  $b = [1\bar{1}0]$  screw superdislocation dissociated on the (111) plane. The shear stress is applied parallel to this plane in the  $[1\bar{1}0]$  direction. The dislocation core structure and its motion are constantly monitored by the Nye tensor method developed earlier in this work (see below). The results obtained so far can be briefly summarized as follows:

The initial state of the dislocation is a planar core dissociated on (111) with the partials separated by an APB (Fig. 4). Each partial, in turn, is narrowly dissociated in two Shockley partials separated by a CSF. This configuration turns out to be unstable and at finite temperatures quickly transforms to a nonplanar core with the partials dissociated on the secondary octahedral plane ( $11\bar{1}$ ). This dissociation is dynamic: every once in a while the Shockley partials spontaneously recombine and immediately redissociate. Such recombination-dissociation events require a constriction of the CSF and are thermally activated events. Eventually, one or both of the superpartials constrict, cross-slip along the (001) plane by  $b/2$ , and re-dissociate on a (111) plane parallel to the initial one, thus forming a so-called PPV lock [4]. The dissociation plane of the locked partial is again dynamic and can spontaneously switch between (111) and ( $11\bar{1}$ ). This PPV-locked configuration is more stable than the unlocked one, although a few spontaneous unlocking events have been observed. The latter points to a relatively weak character of PPV locks.

When stress is applied to an unlocked dislocation, it begins to glide along the (111) plane. During the “free flight” of the dislocation the separation of the superpartials and the width of the CSFs are significantly smaller than in the standstill state without a stress. After traveling a distance of a few tens of nanometers, the trailing partial forms a PPV lock and stops the dislocation. The dislocation remains locked for a few hundred picoseconds before the trailing partial breaks the lock and the glide continues. Breaking a PPV lock requires a constriction of the Shockley partials and a cross-slip by  $b/2$  along the (001) plane. Overall, the dislocation moves in a stop-and-go manner (“jerkey motion”) caused by repeated PPV locking and unlocking events (Fig. 5). Although the average dislocation velocity (100-200 m/s) is much smaller than for the velocity of free glide, the resistance imposed by the PPV locks is not strong enough to account for the YSA. Furthermore, this resistance decreases with temperature since the unlocking process is assisted by temperature.

After a few nanoseconds of stop-and-go motion, the dislocation stops due to the formation of a much stronger lock than PPV, which blocks its motion for the rest of the simulation. Namely, in the process of unlocking of a PPV configuration, the constricted trailing partial “misses” the primary (111) plane and continues to glide along the (001) cube plane by a few more Burgers vectors before it stops and dissociates into Shockley partials in an octahedral plane. Subsequently, it may advance along the (001) plane somewhat further whereas the leading partial continues to be on the (111) plane. This creates a highly stable angular configuration.

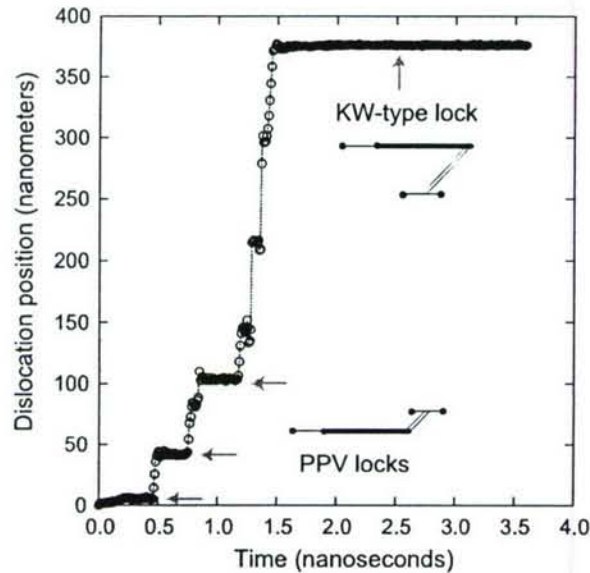


Figure 5: Position of the  $\langle 110 \rangle$  screw superdislocation as a function of time in MD simulation at the temperature of 1000 K under a shear stress of 700 MPa. The dislocation first moves by a stop and go mechanisms by the formation and destruction of PPV locks. After 1.5 ns it stops due to the formation of an incomplete KW lock and remains immobilized until the end of the simulation.

It is pulled forward by the Peach-Koehler forces acting on both partials but is pinned by the intersection line of the (111) and (001) APBs. This configuration can only unlock if the leading partial moves back to the APB intersection, which requires work against the Peach-Koehler force.

This sessile configuration can be viewed as a new form of a Kear-Wilford (KW) lock. Its formation is associated with a large thermal activation (multiple constrictions of the CSF). Our simulations suggest that this lock may be responsible for the immobilization of dislocations in  $\text{Ni}_3\text{Al}$  and thus the increase of its strength with temperature. The loss of strength beyond the peak temperature is likely to be caused by the thermally activated unlocking of such configurations and initiation of cubic slip. In the ongoing work, we are continuing to study the dislocation locking mechanisms in a more systematic manner by analyzing the trends across different temperatures and stresses.

## 6 The Nye tensor method for dislocation characterization

A new method of presentation of dislocation core structure by a distribution of its Nye tensor components has been developed [5]. This method is based on the concept of a continuously dislocated crystal which represents the misfit due to a dislocation by a distribution of infinitesimal dislocations [6–8]. The infinitesimal Burgers vector  $db$  of the continuously distributed

dislocations crossing a small area  $dS$  with a unit normal  $\mathbf{n}$  is given by  $d\mathbf{b} = \boldsymbol{\alpha} \cdot \mathbf{n} \cdot dS$ ,  $\boldsymbol{\alpha}$  being the Nye tensor. A computer program has been developed that calculates the Nye tensor distribution over a chosen plane given atomic coordinates in a dislocated crystal and the perfect lattice orientation. This distribution is represented by contour plots of individual Nye tensor components. The peaks of the distribution represent full or partial dislocation. The sign of the relevant Burgers vector component can be immediately determined from the sign of the respective component of  $\boldsymbol{\alpha}$ . Furthermore, by integrating the distribution of  $\boldsymbol{\alpha}$  over a peak area all components of the Burgers vector of the dislocation can be determined with high accuracy. It has been demonstrated that this method is insensitive to lattice distortions other than those associated with dislocation cores, which makes its spatial resolution much higher than with other methods. As an illustration, Figure 6 shows the structure of a  $\langle 110 \rangle$  screw superdislocation in  $\text{Ni}_3\text{Al}$  dissociated with the formation a  $(111)$  APB. Each superpartial is observed to dissociate into closely separated Shockley partials on a non-coplanar  $\{111\}$  plane. The plot does not display the GSFs in order to enhance the clarity of visualization of the partial dislocations.

The Nye tensor method has been applied to the interpretation of high-resolution electron microscopy images of screw dislocations in Mo [9]. It has been demonstrated that Nye tensor plots of the images “wash out” the effect of the Eshelby twist and give a more informative presentation of the core structure than other methods can do.

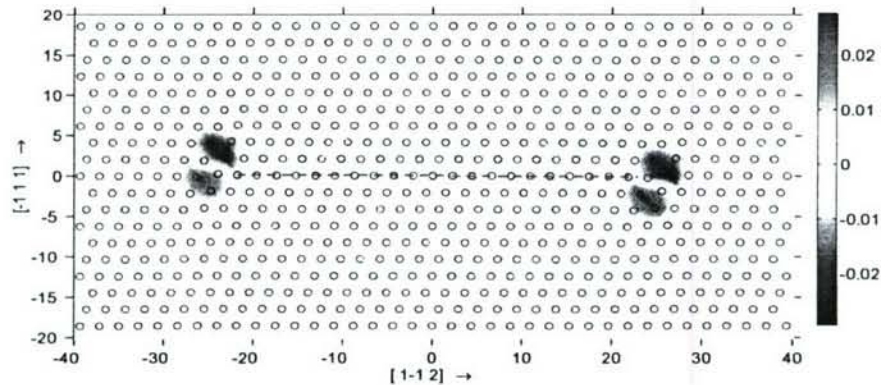


Figure 6: Nye plot of a  $\langle 110 \rangle$  screw dislocation in  $\text{Ni}_3\text{Al}$  after a molecular dynamics run at 500 K. The contour plot shows the Nye tensor component parallel to the dislocation line and to the  $[112]$  direction. The dashed line was drawn by hand to outline the  $(111)$  APB. The brown and blue peaks identify the Shockley partials and indicate the signs of their  $[112]$  components. The distances are in  $\text{\AA}$  and the Nye tensor in  $1/\text{\AA}$ .

## 7 Publications and conference presentations

The following publications resulted from this project and contain a specific acknowledgement of this grant:

1. A. Y. Lozovoi and Y. Mishin: Point defects in NiAl: The effect of lattice vibrations, *Physical Review B*, 2003, **68**, p. 184113.
2. R. R. Zope and Y. Mishin: Interatomic potentials for atomistic simulations of the Ti-Al system, *Physical Review B*, 2003, **68**, p. 024102.
3. Y. Mishin: Atomistic modeling of the gamma and gamma' phases of the Ni-Al system, *Acta Materialia*, 2004, **52**, p. 1451-1467.
4. C. S. Hartley and Y. Mishin: Representation of dislocation cores using Nye tensor distributions, *Materials Science and Engineering A*, 2005, **400**, pp. 18-21.
5. Y. Mishin, I. V. Belova and G. E. Murch: Atomistic modeling of diffusion in the TiAl compound, *Defect and Diffusion Forum*, 2005, **237-240**, pp. 271-276.
6. C. S. Hartley and Y. Mishin: Visualization and characterization of the lattice misfit associated with dislocation cores, *Acta Materialia*, 2005, vol. 53, pp. 1313-1321.
7. Y. Mishin: Atomistic computer modeling of intermetallic alloys, *Materials Science Forum*, 2005, **502**, pp. 21-26.
8. Y. Mishin: Atomistic Computer Simulation of Diffusion, Chapter 3 in *Diffusion Processes in Advanced Technological Materials* (edited by D. Gupta), pp. 113-172, Noyes Publications/William Andrew, NY, 2005.
9. B. G. Mendis and Y. Mishin and C. S. Hartley and K. J. Hemker: Use of the Nye tensor in analysing HREM images of bcc screw dislocations, *Philosophical Magazine*, 2006, **86**, pp. 4607-4640..

The results of this project have been reported in the following conference presentations:

1. Y. Mishin: Atomistic Modeling of Diffusion, Sixth International Conference on Diffusion in Materials, 18-23 July 2004, Krakow, Poland. [Invited talk]
2. Y. Mishin, I. V. Belova and G. E. Murch: Atomistic Modeling of Diffusion in the TiAl Compound, Sixth International Conference on Diffusion in Materials, 18-23 July 2004, Krakow, Poland.
3. Y. Mishin: Atomistic modeling of high-temperature structural aluminides, Symposium on Materials by Design: Atoms to Applications, TMS Annual Meeting, Charlotte, NC, March 14-18, 2004. [Invited talk]

4. Y. Mishin: Atomic computer simulation of advanced intermetallic alloys. International Conference on New Frontiers of Process Science and Engineering in Advanced Materials (PSEA'04), Kyoto, Japan, November 24-26, 2004. [Invited talk]
5. B. G. Mendis and Y. Mishin and C. S. Hartley and K. J. Hemker: HREM imaging of screw dislocation core structures in bcc metals, Symposium on Electron Microscopy of Molecular and Atom-Scale Mechanical Behavior, Chemistry, and Structure, MRS Fall Meeting, Boston, MA, November 29 – December 3, 2004.
6. C. S. Hartley and Y. Mishin: Representation of dislocation cores using Nye tensor distributions. International Conference on the Fundamentals of Plastic Deformation (Dislocations 2004), French Riviera, France, September 13-17, 2004.
7. Y. Mishin: Effective diffusivity of heterogeneous systems, Symposium on Multicomponent Multiphase Diffusion, TMS Annual Meeting, San Francisco, CA, February 13-17, 2005. [Invited talk].

## References

- [1] Mishin, Y., *Acta Mater.*, 2004, **52**, 1451.
- [2] Mishin, Y., Lozovoi, A. Y. and Alavi, A., *Phys. Rev. B*, 2003, **67**, 014201.
- [3] Lozovoi, A. Y. and Mishin, Y., *Phys. Rev. B*, 2003, **68**, 184113.
- [4] Vitek, V., Pope, D. P. and Bassani, J. L., in: *Dislocations in Solids*, edited by F. R. N. Nabarro and M. S. Duesbery, Elsevier/North-Holland, Amsterdam, 1996 136, vol. 10.
- [5] Hartley, C. S. and Mishin, Y., *Acta Mater.*, 2005, **53**, 1313.
- [6] Nye, J. F., *Acta Metall.*, 1953, **1**, 153.
- [7] Bilby, B. A., in: *Bristol Conference Report on Defects in Crystalline Materials*, Physical Society, London, 1955 123.
- [8] Bilby, B. A., in: *Progress in Solid Mechanics*, edited by I. N. Sneddon and R. P. Hill, volume 1, 1960 330–398.
- [9] Mendis, B. G., Mishin, Y., Hartley, C. S. and Hemker, K. J., 'Use of the nye tensor in analysing HRTEM images of bcc screw dislocations,' *Philos. Mag.*, in press.